Swansea University
Prifysgol Abertawe

Cronfa
Setting Research Free

Cronfa - Swansea University Open Access Repository

This is an author produced version of a paper published in:
IEICE Transactions on Information and Systems

Cronfa URL for this paper:
http://cronfa.swan.ac.uk/Record/cronfa51640

Paper:
MAN, D., W. JONES, M., LI, D., ZHANG, H. & SONG, Z. (2019). Calibration of Turntable Based 3D Scanning Systems. *IEICE Transactions on Information and Systems, E102.D*(9), 1833-1841.
http://dx.doi.org/10.1587/transinf.2019EDP7043

This item is brought to you by Swansea University. Any person downloading material is agreeing to abide by the terms of the repository licence. Copies of full text items may be used or reproduced in any format or medium, without prior permission for personal research or study, educational or non-commercial purposes only. The copyright for any work remains with the original author unless otherwise specified. The full-text must not be sold in any format or medium without the formal permission of the copyright holder.

Permission for multiple reproductions should be obtained from the original author.

Authors are personally responsible for adhering to copyright and publisher restrictions when uploading content to the repository.

http://www.swansea.ac.uk/library/researchsupport/ris-support/

PAPER

Calibration of Turntable Based 3D Scanning Systems

Duhu MAN[†a)], ***Member***, **Mark W. JONES**[†b)], **Danrong LI**[††c)], **Honglong ZHANG**[†††d)], ***and*** **Zhan SONG**[†††e)], ***Nonmembers***

SUMMARY The consistent alignment of point clouds obtained from multiple scanning positions is a crucial step for many 3D modeling systems. This is especially true for environment modeling. In order to observe the full scene, a common approach is to rotate the scanning device around a rotation axis using a turntable. The final alignment of each frame data can be computed from the position and orientation of the rotation axis. However, in practice, the precise mounting of scanning devices is impossible. It is hard to locate the vertical support of the turntable and rotation axis on a common line, particularly for lower cost consumer hardware. Therefore the calibration of the rotation axis of the turntable is an important step for the 3D reconstruction. In this paper we propose a novel calibration method for the rotation axis of the turntable. With the proposed rotation axis calibration method, multiple 3D profiles of the target scene can be aligned precisely. In the experiments, three different evaluation approaches are used to evaluate the calibration accuracy of the rotation axis. The experimental results show that the proposed rotation axis calibration method can achieve a high accuracy.

key words: *3D model, laser plane acquisition, point cloud registration, turntable calibration, least squares optimization*

1. Introduction

A 3D model of a real-world object can be constructed by capturing multiple partial scans of the object from different view points and then aligning them into a consistent coordinate system. One approach to obtaining multiple scans is to use a hand-held scanner to scan a fixed object, but this can cause a registration problem because of unstable scanning motion. A more stable approach is to use a turntable to rotate the object itself or camera to acquire different parts of the object. Brown et al. [4] used a turntable based scanning system to acquire 3D geometry of archaeological wall painting fragments. Li et al. [10] introduced a turntable based 3D scanning system to study plant growth, particularly focusing on accurate localization and tracking topological events like budding and bifurcation. More recently, along with the popularity of consumer-level 3D printers, the demand for low-cost 3D scanners is increasing significantly. To meet this requirement, 3D scanning systems comprising line-laser emitter, mobile phone (with camera) and turntable are now popular [1], [2]. Using a turntable has many advantages, including easy installation, good stability, and low registration cost. Once the turntable axis is calibrated, the scan sequence of any object can be easily integrated into a complete model by rotating the partial scans around the calibrated turntable axis, without suffering from interference caused by noise, outliers, low degrees of overlap, and so on.

The commonly used combinations of camera and turntable are shown in follows:

Combination 1. As shown in Fig. 1, the camera is fixed and the object for scanning will be placed on the turntable. The partial scans of the object are captured by rotating the turntable. The calibration of the turntable in this combination has been extensively studied by researchers. Rushmeier et al. [16] proposed an approach to calibrate the turntable by placing a pin-registered 45-degree plane onto the turntable. The target is scanned at three different turntable positions. The rotation axis is then found by taking the intersection of the three planes. Soon-Yung Park and Murali Subbarao [14] used a checkerboard as a calibration tool to estimate the rotation axis. Their approach involves computing the 3D positions of corner points on the checkerboard in different scans and solving an over-determined linear equation to approximate the axis direction. Li et al. [3] used a criterion sphere mounted on the turntable as a calibration tool. They captured a circle fitted to the center of the sphere at different angles by rotating the turntable. They then used a different-sized sphere to obtain another circle and defined the rotation axis as the line joining the centers of the two circles.

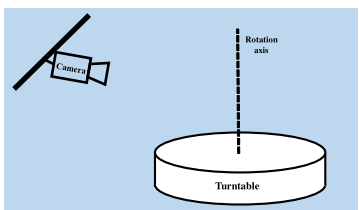

Fig. 1 Combination 1

Manuscript received February 14, 2019.
Manuscript publicized May 30, 2019.

[†]The authors are with the Department of Computer Science, Swansea University, Singleton Park, Swansea SA2 8PP, United Kingdom.

[††]The author is with the University of Science and Technology of China, No.96, JinZhai Road Baohe District, Hefei, Anhui, 230026, P.R.China.

[†††]The authors are with the Shenzhen Institutes of Advanced Technology, Chinese Academy of Sciences, 1068 Xueyuan Avenue, Shenzhen University Town, Shenzhen, P.R.China.

a) E-mail: m.duhu@swansea.ac.uk
b) E-mail: m.w.jones@swansea.ac.uk
c) E-mail: sa615495@mail.ustc.edu.cn
d) E-mail: hl.zhang1@siat.ac.cn
e) E-mail: zhan.song@siat.ac.cn

DOI: 10.1587/transinf.2019EDP7043

Copyright © 2019 The Institute of Electronics, Information and Communication Engineers

Ye et al. [17] set a pattern perpendicular to the turntable to calibrate the rotation axis, and calculated the turntable axis with respect to the fixed camera coordinate frame. Chen et al. [5] proposed a method in which a checkerboard plate is placed on a turntable and photos of 3D corner points of checkerboard pattern is taken from a 360-degree viewpoint. The circular-trajectory plane equation of the retrieved corner points is then computed and the normal vector along the rotation axis is calculated by using the least square method. Pang et al. [13] proposed a tool-free method to automatically calibrate the turntable axis directly from the 3D scan sequence of the input object. Their method first registers a pair of 3D scanned points to recover the initial turntable axis. The turntable axis is then optimized by iteratively approximating a rotation matrix to the refined registration matrix.

Combination 2. As shown in Fig. 2, the camera is mounted on the top of the turntable. The camera turns around the rotation axis when the turntable is rotating. This combination can be used to reconstruct an environment in which camera is placed (for example, a full room scene). However, the rotation axis calibration methods mentioned above are not suitable for this combination, since the camera is moving and it cannot see the rotation axis. Few turntable calibration methods have been proposed for this combination so far. Niu et al. [12] proposed a method in which two cameras and two checkerboards were used. It means users need to have at least two cameras even if the scanning system itself just needs one camera. In this paper, we propose a simple method for the turntable calibration of this combination. The proposed method just uses the scanning system itself and a checkerboard to implement the calibration. The proposed method can be applied to general turntable-based scanning systems, including the system is with one camera. Our discussion is based on the use of a line laser scanning system that consists of a camera, a laser projector and a turntable.

3D scanning systems comprising line-laser projector, camera and turntable have been presented that are able to produce 3D points for 360 degree viewing from image sequences. In [7], Konolige et al. proposed a 3D distance measurement system which consists of a laser emitter, a camera and a turntable, to acquire 3D information of indoor environments. Gao et al. [6] introduced a simple system just comprising laser emitter and mobile phone (with camera) for the applications in outdoor environments. They pointed out that their system can be combined with a turntable to acquire a complete 3D information of the environment. However these papers have no explanation about the point cloud registration and the accurate calibration of turntable.

This paper is an extension of our previous work [9]. The major additions are:

- The calibration method shown in this paper can calibrate the turntable with any rotation angle, even the rotation angle is very small. However, the method presented in [9] can only calibrate the turntable with larger rotation angle.
- In this paper, we show details for the localization of laser center.
- In this paper, we present a new evaluation method for checking the accuracy of the turntable calibration.

2. Experimental Setup

We implement the proposed calibration method on a turntable based laser scanning system. The diagram of the experimental system is shown in Fig. 3. The line-laser projector and camera are fixed and mounted on the turntable. During scanning, the line-laser projector remains open, the turntable starts from a position with angle of 0 degree, and images with the laser-line are captured every α degrees. The 3D coordinate of the point cloud of the intersecting line of the laser plane and the surface of the objects is calculated under the current camera coordinate frame. The turntable rotates $360/\alpha$ times to complete a full scan. With the rotation axis calibrated, point clouds computed at various scanning positions can be registered to a unique coordinate system. The synchronization between the turntable, camera and laser projector is controlled by the synchronizor which consists of a single-chip controller and a electrical relay.

3. Laser Line Extraction

The brightness of the cross-section of the laser beam follows the Gaussian distribution, thus it is possible to utilize Gaussian profile fitting to detect the laser line center. Matiukas and Miniotas [11] use two shifted kernels of the first order Gaussian derivatives to detect the left and right edges of the laser line, then a nonlinear combination of these two filters

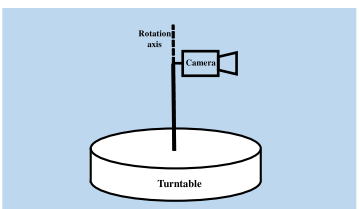

Fig. 2 Combination 2

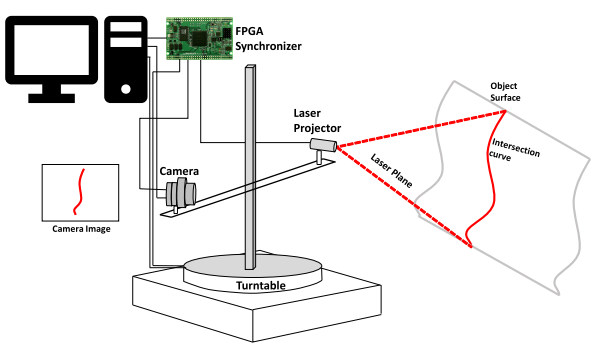

Fig. 3 Structure of experimental 3D laser scanning system.

is used for further computation of laser line center. Our laser line extraction method is based on their algorithm.

The left and right edge detectors are designed as follows:

$$\begin{aligned} E_L(x,y) &= -G'_\sigma(x+s,y) \\ E_R(x,y) &= G'_\sigma(x-s,y) \end{aligned} \tag{1}$$

where $G'_\sigma(x\pm s,y)$ denotes the shifted kernels of the first order Gaussian derivatives; (x,y) represents the coordinate of pixel in the image; σ is the data variation of the Gaussian distribution. For simplicity, we take $\sigma = s$ and the calculation of s depends on the width of the laser line profile w. Here we let $s = 0.4482w$. These two edge detectors combined, as follows, to detect the bar-like structure in the input image I.

$$F(x,y) = min[pos(E_L \otimes I)(x,y), pos(E_R \otimes I)(x,y)], \tag{2}$$
$$s.t. pos\{\mu\} = \begin{cases} \mu, \mu > 0 \\ 0, \text{otherwise} \end{cases}$$

The center line of the laser beam is calculated from the local maxima in the filtered image. The local maxima correspond to the first and second order derivatives of the filtered image. In our implementation, for detecting a laser beam with different width, we use 4 different scales for the filters with varying σ.

4. Calibration of Camera and Laser Plane

The 3D reconstruction system presented in this paper is based on the pinhole camera model. As shown in Fig. 4, a point in the world coordinate frame can be transformed to the camera coordinate frame, then to the image frame. The relation between a 2D image point, $P_i(u,v)$ and a 3D world point, $P_w(x_w,y_w,z_w)$ can be expressed:

$$\begin{bmatrix} u \\ v \\ 1 \end{bmatrix} = A \begin{bmatrix} R & t \end{bmatrix} \begin{bmatrix} x_w \\ y_w \\ z_w \\ 1 \end{bmatrix}$$
$$with\ A = \begin{bmatrix} \alpha & \gamma & u_0 \\ 0 & \beta & v_0 \\ 0 & 0 & 1 \end{bmatrix} \tag{3}$$

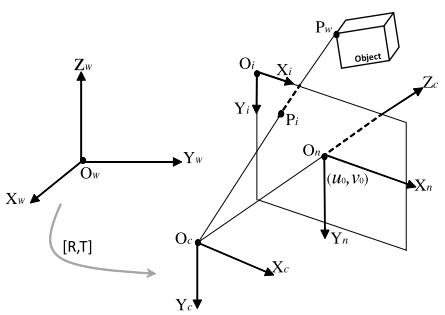

Fig. 4 Geometrical model of the 3D scanning system, where O_w-$X_wY_wZ_w$: world coordinate frame, O_c-$X_cY_cZ_c$: camera coordinate frame, O_i-X_iY_i: image coordinate frame, O_n-X_nY_n: normalized image coordinate frame.

where (R,t), the extrinsic parameters of camera, are the rotation and translation which relate the world coordinate frame to the camera coordinate frame, and A is called the camera intrinsic matrix where (u_0,v_0) are the coordinates of the principal point of camera in the image coordinate frame, α and β are the scale factors along with X_i and Y_i axes in the image coordinate frame and γ is the parameter describing the skew of the two image axes. The extrinsic parameters (R,t) can be expressed by the following 4×4 matrix.

$$\begin{bmatrix} R & t \end{bmatrix} = \begin{bmatrix} r_{1,1} & r_{2,1} & r_{3,1} & t_x \\ r_{1,2} & r_{2,2} & r_{3,2} & t_y \\ r_{1,3} & r_{2,3} & r_{3,3} & t_z \\ 0 & 0 & 0 & 1 \end{bmatrix} \tag{4}$$

4.1 Camera Calibration

For the calibration of camera parameters including distortion coefficients, Zhang [19] proposed a flexible and high precision approach requiring only a camera to observe a planner pattern which can be printed and placed on a rigid planar surface shown at a few different orientations. Our camera calibration follows Zhang's method.

When considering lens distortion of camera, there are deviations between the actual projection points (u',v') and the theoretical projection points (u,v) in the image [8]. For most lenses, the distortion model can be approximated as:

$$\begin{cases} u' = u(1+k_1r^2+k_2r^4) + 2p_1uv + p_2(r^2+2u^2) \\ v' = v(1+k_1r^2+k_2r^4) + p_1(r^2+2v^2) + 2p_2uv \end{cases} \tag{5}$$

where $r^2 = u^2+v^2$, k_1 and k_2 are the coefficients of radial distortion, p_1 and p_2 are the coefficients of tangential distortion.

4.2 Laser Plane Acquisition

In the camera coordinate frame, the laser plane can be formulated as:

$$ax_c + by_c + z_c = c \tag{6}$$

where a, b and c are correlations describing the laser plane. Then the 3D coordinate of an image point (u,v) can be determined by Eqs. (3) and (6) jointly. For solving the laser plane equations, at least three non-collinear 3D points in the camera coordinate frame are needed.

During camera calibration, each calibration plate with different orientations corresponds to a group of extrinsic parameter (R,t). If we irradiate the laser beam on the calibration plates with different orientations, a group of 3D points without a linear relation can be computed. More specifically, according to Zhang's calibration method, the calibration plate is on $Z = 0$ of the world coordinate frame, therefore with the image coordinates of laser line, Eq. (6) can be solved, where the laser line can be extracted with the method proposed in Sect. 3. With a number of image points (u_k,v_k), $k = 1,2,3,\ldots,n$, on the laser line, the corresponding 3D

points (x_k, y_k, z_k) under the camera coordinate frame can be calculated using the following equations:

$$z_k = \frac{r_{31}t_x + r_{32}t_y + r_{33}t_z}{(u_k - u_0)r_{33}/\alpha + (v_k - v_0)r_{32}\beta + r_{33}} \tag{7}$$

$$y_k = \frac{z_k(v_k - v_0)}{\beta} \tag{8}$$

$$x_k = \frac{z_k(u_k - u_0) - \gamma y_k}{\alpha} \tag{9}$$

where $r_{3,1}$, $r_{3,2}$, $r_{3,3}$ and t_x, t_y, t_z are corresponding elements of the rotation matrix and translation vector. Moreover, the laser plane can be fitted by using a series of laser lines on the calibration plates with different orientations.

$$\min_{a,b,c} \left\| \begin{pmatrix} x_1 & y_1 & 1 \\ \vdots & \vdots & \vdots \\ x_n & y_n & 1 \end{pmatrix} \begin{pmatrix} a \\ b \\ c \end{pmatrix} - \begin{pmatrix} z_1 \\ \vdots \\ z_n \end{pmatrix} \right\|^2 \tag{10}$$

By solving Eq. (10) via the known least squares method, the constants a, b and c can be uniquely identified.

5. Turntable Calibration

The proposed turntable calibration method consists of three phases. In the first phase, the transformation matrix of two cameras in different positions is computed. In the second phase, a fitting circle is computed using the result of the first phase. In the third phase, many similar fitting circles are obtained and the rotation axis is computed using centers of those fitting circles.

5.1 Phase 1: Trasformation Matrix Computation

While the turntable of the scanning system is rotated, the obtained multiple 3D laser lines should be aligned together under the same coordinate frame. We select the camera coordinate frame of the starting position of turntable as the unique coordinate frame. If the installation of the scanning system is precise, the rotation axis will coincides with the vertical support of the turntable, then the camera coordinate frame also rotates around the vertical support of the turntable as shown by Fig. 5. The transformation matrix between $O_{c0}\_X_{c0}Y_{c0}Z_{c0}$ and $O_c\_X_cY_cZ_c$ can be obtained using Rodrigues rotation formula [15].

In practice, it is impossible to obtain the ideal mount of bracket and camera. The camera coordinate frame doesn't revolve around the vertical support but around the rotation axis. It is difficult to estimate the transformation matrix between $O_{c0}\_X_{c0}Y_{c0}Z_{c0}$ and $O_c\_X_cY_cZ_c$. On the other hand, from the camera calibration, we know that the transformation matrix which relates the world coordinate frame to the camera coordinate frame was obtained after camera calibration. Therefore if two cameras located at O_{c0} and O_c take a picture from a fixed calibration plate respectively, as shown in Fig. 6, we can get their transformation matrix as:

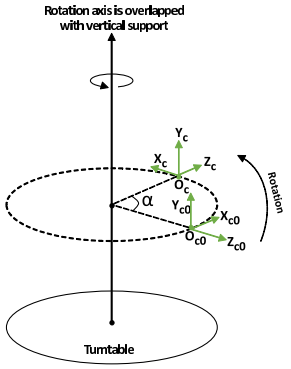

Fig. 5 Scanning system with precise installation, the rotation axis coincides with the vertical support.

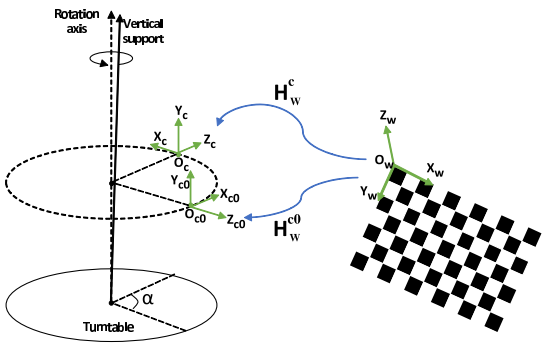

Fig. 6 Scanning system with mounting error, the rotation axis does not coincide with the vertical support; the transformation matrix between two cameras can be obtained by a fixed calibration plate.

$$\begin{bmatrix} X_{c0} \\ Y_{c0} \\ Z_{c0} \\ 1 \end{bmatrix} = H_w^{c0} \begin{bmatrix} X_w \\ Y_w \\ Z_w \\ 1 \end{bmatrix}, with\ H_w^{c0} = \begin{bmatrix} R & t \\ 0^T & 1 \end{bmatrix}_w^{c0} \tag{11}$$

$$\begin{bmatrix} X_c \\ Y_c \\ Z_c \\ 1 \end{bmatrix} = H_w^{c} \begin{bmatrix} X_w \\ Y_w \\ Z_w \\ 1 \end{bmatrix}, with\ H_w^{c} = \begin{bmatrix} R & t \\ 0^T & 1 \end{bmatrix}_w^{c} \tag{12}$$

$$\begin{bmatrix} X_c \\ Y_c \\ Z_c \\ 1 \end{bmatrix} = H_w^{c} H_w^{c0-1} \begin{bmatrix} X_{c0} \\ Y_{c0} \\ Z_{c0} \\ 1 \end{bmatrix} = Tr \begin{bmatrix} X_{c0} \\ Y_{c0} \\ Z_{c0} \\ 1 \end{bmatrix} \tag{13}$$

The transformation matrix corresponds to the unit angle α can be obtained using Eqs. (11)-(13). For a given angle $a = n \times \alpha$ ($n = 0, 1, 2, \ldots, \lfloor 360/\alpha \rfloor$), the camera coordinate frame can be transformed to the unique coordinate frame as:

$$\begin{bmatrix} X_{cn} \\ Y_{cn} \\ Z_{cn} \\ 1 \end{bmatrix} = Tr^n \begin{bmatrix} X_{c0} \\ Y_{c0} \\ Z_{c0} \\ 1 \end{bmatrix} \tag{14}$$

To improve the computation speed, Tr^n is stored as a look-up-table. The scanning system can reconstruct the laser line at every α degrees, and with the global registration, a complete 3D model of the scene can be obtained.

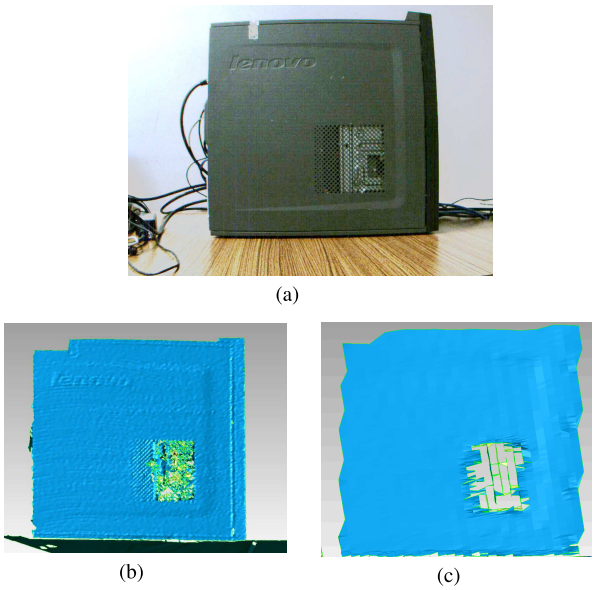

Fig. 7 Qualities of reconstructions with different rotation angles. (a) Computer box for scanning; (b) reconstruction with rotation angle of 0.1°; (c) reconstruction with rotation angle of 1°.

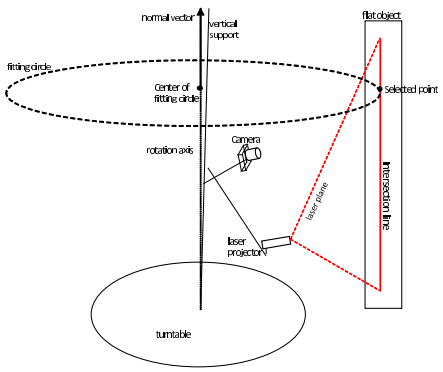

Fig. 8 Illustration of the calibration of rotation axis with fitting circle.

5.2 Phase 2: Rotation Axis Calibration

In practice, a smaller rotation angle (unit angle) will generate a higher quality of 3d reconstruction, see Fig. 7. However, the registration method shown in Sect. 5.1 will fail when the unit angle α is too small or changes during the reconstruction procedure. If the unit angle α is too small, for example 0.1°, the position change of camera is not significant and it is hard to obtain the transformation matrix Tr exactly. Therefore, the rotation axis should be calibrated.

As shown in Fig. 8, a laser line is irradiated on a flat object and reconstructed using the camera model and laser plane equation. A point is selected from the reconstructed laser line and transformed n times using transformation matrix Tr where we set the unit rotation angle $\alpha = 1°$ and $n = 360$. The trajectory of the transformed points is a circle and its center is located on the rotation axis. We call this circle, the fitting circle, its center, radius and normal vector can be computed in the following four steps. First, we fit a plane using those points on the trajectory circle, where the plane fitting method described in Sect. 4.2 is used. Second, we use the Rodrigues rotation formula to project the 3D trajectory points onto the fitting plane and get their 2D X-Y coordinate in the coordinate system of the plane. The Rodrigues rotation formula is shown in Eq. (15), where P and P_{rot} represent the points before and after rotation, respectively, θ is rotation angle, k is a unit vector describing an axis of rotation. We choose axis of rotation k as cross product between plane normal and normal of the new X-Y coordinate.

$$P_{rot} = Pcos(\theta) + (k \times P)sin(\theta) + k(k \cdot P)(1 - cos(\theta)) \quad (15)$$

Third, we fit a circle in 2D X-Y coordinate. In 2D space, a circle with radius r and center $(x_c, y_c)^T$ can be formulated as:

$$\begin{aligned} (x - x_c)^2 + (y - y_c)^2 &= r^2 \\ (2x_c)x + (2y_c)y + (r^2 - x_c^2 - y_c^2) &= x^2 + y^2 \\ c_0 x + c_1 y + c_3 &= x^2 + y^2 \end{aligned} \quad (16)$$

where we introduced a vector $c = (c_0, c_1, c_3)^T$ ($c_0 = 2x_c$, $c_1 = 2y_c$, $c_3 = r^2 - x_c^2 - y_c^2$) for unknown parameters. Applied to all projected points, it yields to a system of linear equations

$$Ac = b \quad (17)$$

where

$$A = \begin{pmatrix} x_1 & y_1 & 1 \\ \vdots & \vdots & \vdots \\ x_n & y_n & 1 \end{pmatrix}, \; b = \begin{pmatrix} x_1^2 + y_1^2 \\ \vdots \\ x_n^2 + y_n^2 \end{pmatrix} \quad (18)$$

Since we have more equations than unknowns, we can find a solution by method of least-squares as described in Sect. 4.2, which minimizes the square sum of residuals $\|b - Ac\|^2$. Finally we use the Rodrigues rotation formula again to transform 2D circle center to 3D coordinate.

According to Rodrigues rotation formula, the normal vector of the plane and 3D circle center can be used to compute the transformation matrix between two cameras with different positions around the rotation axis. As shown in Fig. 9, when the camera moves from position O_{c0} to O_c around the rotation axis with rotation angle θ, the transformation matrix can be expressed as follows:

$$\begin{pmatrix} R(\tilde{n}, \theta) & (I - R(\tilde{n}, \theta))\tilde{C} \\ 0 & 1 \end{pmatrix} \quad (19)$$

$$with \;\; R(\tilde{n}, \theta) = I + sin\theta[\tilde{n}]_\times + (1 - cos\theta)[\tilde{n}]_\times^2$$

$$where \;\; [\tilde{n}]_\times = \begin{bmatrix} 0 & -\tilde{n}_z & \tilde{n}_y \\ \tilde{n}_z & 0 & -\tilde{n}_x \\ -\tilde{n}_y & \tilde{n}_x & 0 \end{bmatrix}$$

where $C(x_{cc}, y_{cc}, z_{cc})^T$ is the coordinate of the center of the fitting circle and $\tilde{C}$ is its homogeneous expression such that $\tilde{C} = C(x_{cc}, y_{cc}, z_{cc}, 1)^T$. The normalized normal vector is

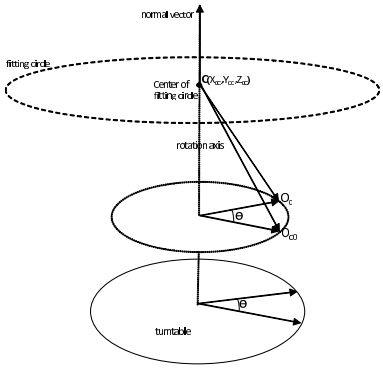

Fig. 9 Illustration of transformation between cameras with different positions using Rodrigues rotation formula.

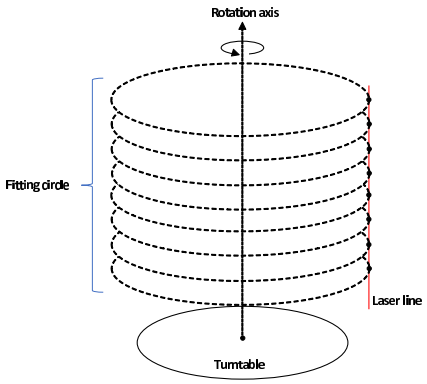

Fig. 10 The rotation axis fitted by centers of circles.

noted by $n(n_x, n_y, n_z)$ and its homogeneous expression is $\tilde{n}(\tilde{n}_x, \tilde{n}_y, \tilde{n}_z)$.

5.3 Phase 3: Optimization

In phase 2, only one fitting circle is computed and used to calibrate the rotation axis. However we can obtain many such fitting circles by selecting different points from the reconstructed laser line, see Fig. 10. In general, the rotation axis passes through centers of all the circles. Therefore, the rotation axis can be fitted by those center points. A least-squares line fitting algorithm [18] is used to fit the rotation axis.

6. Evaluation

In this section, the calibration results for the camera, laser plane and rotation axis are described first. Then three different evaluation methods are proposed to evaluate the rotation axis calibration method proposed.

The experimental setup consists of a USB 3.0 camera with resolution of 1280×1024 pixels, and a lens with a 6*mm* focal length. A red line laser with an emitting angle of about 90 degree is used. After installing the scanning system, the camera can be calibrated using the method of Zhang. The calibration takes a total of 23 calibration plate images, of which the last four are used to fit the laser plane equation.

Table 1 Intrinsic parameters

Parameters	α	β	u_0	v_0
Values	2894.462	2887.338	1016.814	817.261

Table 2 Laser plane coefficients

Laser Plane Coefficients	a	b	c
Value	−7.606	−1.685	1296.203

Table 3 Direction vector and base point (arbitrarily selected) of the rotation axis

Parameters	Estimated value
Direction vector (n_x, n_y, n_z)	(−0.0040, 0.9805, 0.1960)
Base point (x, y, z)	(−49.589, 997.523, 1209.365)

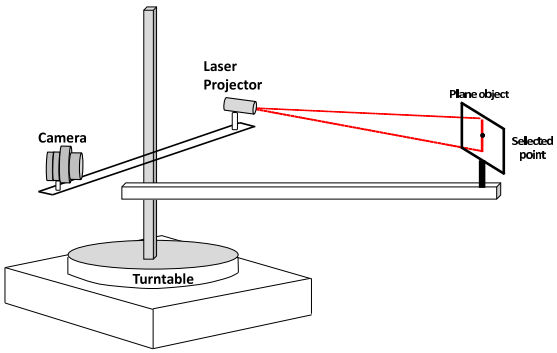

Fig. 11 The mount of plane object to the scanning system.

The last two are used to estimate the rigid transformation matrix of cameras before and after rotation. The intrinsic matrix A and the transformation matrix Tr obtained by the calibration of camera are shown in Table 1 and the following equation, where α=1°.

$$Tr = \begin{pmatrix} 0.9994 & 4.0e-005 & -0.0345 & -7.3403 \\ -1.845e-005 & 0.9999997 & 0.00063 & 3.1e-006 \\ 0.03458 & -0.00063 & 0.99940 & 0.21142 \\ 0 & 0 & 0 & 1 \end{pmatrix}$$

During camera calibration procedure, we irradiate the laser beam on the last four calibration plates and extract the centers of each laser beam as laser line. According to the Eqs. (7)-(9), we can get the 3D points (x_k, y_k, z_k) $(k = 1, 2 \ldots n)$ of the laser line under the camera coordinate frame. Then, using these points, Eq. (10) can be solved and the coefficients of the laser plane can be obtained. The laser plane coefficients are shown in Table 2.

The calibration results for the rotation axis are shown in Table 3. In the following subsections, we use three different evaluation methods to evaluate the proposed rotation axis calibration method.

6.1 Evaluation Approach 1

We mount a plane object to the scanning system, see Fig. 11. The relative position of the plane object to the camera and

Table 4 Accuracy evaluation of turntable calibration with markers on a glass wall

	1*st*	2*nd*	3*rd*	4*th*	5*th*	6*th*	7*th*	8*th*	9*th*	10*th*
Distance by reconstruction (mm)	299.26	300.76	299.56	299.60	298.50	300.80	300.19	300.45	299.20	301.18
Deviation (mm)	−0.74	0.76	−0.44	−0.40	−1.50	0.80	0.19	0.45	−0.80	1.18

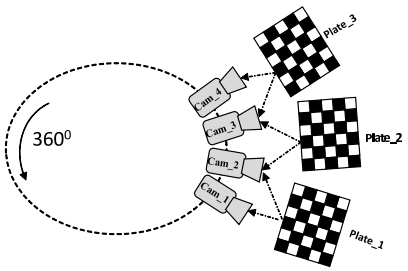

Fig. 12 Computation of transformation matrix of each pair of cameras with a calibration plate

Fig. 13 Flat glass wall with circle markers

laser projector is fixed. We then irradiate a laser line on the plane object and reconstruct it. Select a point from the reconstructed laser line and rotate this point around the rotation axis. The trajectory of the point is a circle and we select 360 points in the circle at each position with 1 degree angle increased. Using the calibrated rotation axis, 3D coordinate of each point can be computed.

Now we use Zhang's calibration method to compute the ground truth. As shown in Fig. 12, the transformation matrix of each pair of cameras can be computed by a calibration plate, for example, the transformation matrix of *Cam_1* and *Cam_2* can be computed by using *Plate_1* and that of *Cam_2* and *Cam_3* can be computed using *Plate_2*, and so on. If we select *Cam_1* as the unique coordinate frame, then all cameras can be mapped into this unique coordinate system. If the angle between two cameras is 1 degree, then the camera will be placed at 360 different positions and the point selected from the laser line can be reconstructed at each position.

The accuracy of the calibration of rotation axis can be evaluated by the following equation, where (x_i, y_i, z_i) is 3D coordinate of the selected laser point at camera position i and it is computed using the rotation axis. The corresponding ground truth is indicated by (x'_i, y'_i, z'_i). The total number of camera positions is indicated by n. The experiment shows that the error can be controlled within $0.5mm$.

$$Error = \frac{\sum_{i=1}^{n} \sqrt{(x_i - x'_i)^2 + (y_i - y'_i)^2 + (z_i - z'_i)^2}}{n} \quad (20)$$

6.2 Evaluation Approach 2

To verify the calibration accuracy of the turntable, a flat glass surface with circle markers is used, see Fig. 13. The diameter of marker is $3cm$. The glass wall has a distance of $\sim 2.5m$ to the camera. The vertical and horizontal ground-truth distance between markers is $300mm$ and it is estimated by a steel ruler manually. By measuring the distance between each pair of neighboring markers with the scanning system and comparing it with the ground truth, the registration accuracy of the scanning system can be evaluated. More specifically, the distance between a pair of markers is estimated using the scanning system as follows: first, we use the least square method to compute the center of each reconstructed marker. Then compute the distance between markers using the obtained centers. The registration accuracy mainly depends on the calibration of the rotation axis. Therefore, if measured distance between markers is very different to the ground truth, it means our rotation axis calibration method is not precise. The experimental results show that, the average measurement error is $0.726mm$, see Table 4.

The planarity of the glass may affect the estimation of ground-truth distance of two markers (it is estimated by steel ruler). Therefore, we have used the reinforced glass to build the glass wall. On the other hand, the distance between two neighbouring markers is only $30cm$, therefore we believe the planarity error can be omitted for two neighbouring markers. However, the planarity of glass has no impact on the reconstruction. Since we always can obtain 3d information of the markers even the glass is not plain enough.

The reconstruction accuracy also depends on the power of laser projector and the focal length of the camera. For the camera (industrial camera) and laser projector used in this work, the maximum reconstruction distance is about $6m$. If the scanning object is within $6m$, the reconstruction error is always smaller than $3cm$. However, if it is larger than $6m$, the error will be increasing significantly. For example, if it is 8m, the error will be larger than $10cm$ because the laser line captured is not clear. However, we can use more powerful laser projector to overcome this defect of the hardware system.

6.3 Evaluation Approach 3

Now we evaluate the proposed method by the reconstruction of a indoor scene. By placing the scanning system in the

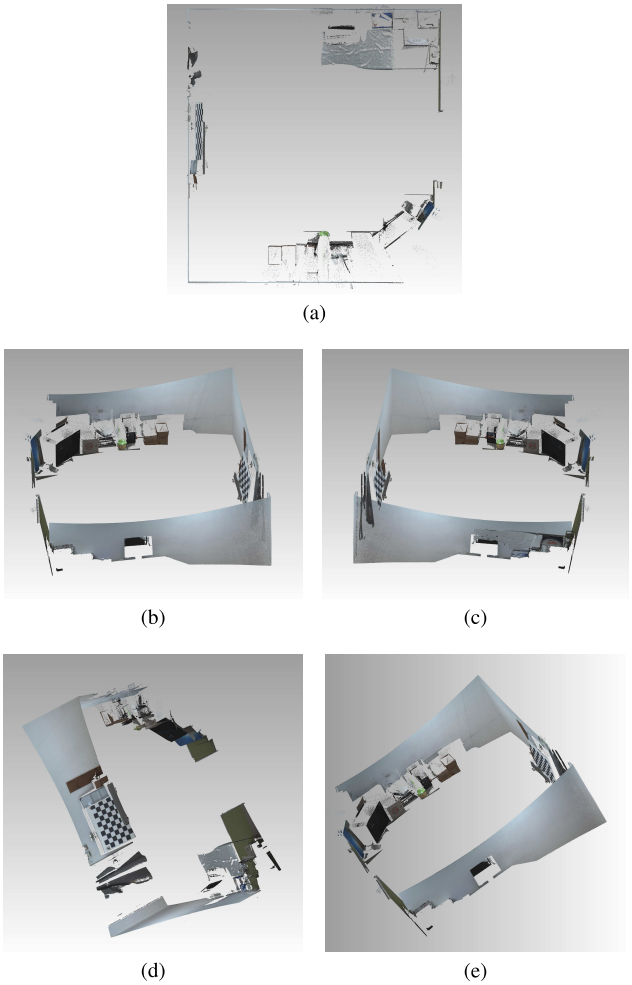

Fig. 14 Reconstructed room scene; (a) top view; (b)(c)(d)(e) side views.

center of a room and rotating it, the dense 3D point cloud of full room scene can be obtained. The size of the room is estimated by a 1D laser range finder and it is $3816mm \times 4652mm$. From the reconstruction results, the measured size of the room is about $3809mm \times 4647mm$. The measurement error can be controlled within $1cm$. The top and side views of the reconstructed room scene is shown in Fig. 14.

7. Conclusion

The consistent alignment of the point clouds obtained from various scanning positions is a crucial step for many 3D modeling systems. This is especially true for environment modeling. In order to observe the full scene, a common approach is to rotate the scanning device around a fixed axis using a turntable. The final alignment of each frame data can be computed from the position and orientation of the rotation axis. This paper presents a novel turntable calibration method. It is evaluated by different evaluation approaches and experimental results show that the proposed method can achieve a high accuracy. Because our proposed method only requires one scan of the scanning object and a calibration plate, it can be applied to any kind of turntable-based scanner, such as stereo-based, structured light-based, or laser.

Acknowledgments

Manduhu is supported by a Sêr Cymru COFUND fellowship.

References

[1] Bevel smartphone 3D scanner, https://3dscanexpert.com/bevel-smartphone-3d-scanner-review/.
[2] Eora 3D scanner, https://eora3d.com/product.
[3] J. Li, M. Chen, X. Jin, Y. Chen, Z. Dai, Z. Ou, and Q. Tang, "Calibration of a multiple axes 3-d laser scanning system consisting of robot, portable laser scanner and turntable," Optik - International Journal for Light and Electron Optics, vol.122, no.4, pp.324–329, 2011.
[4] B.J. Brown, C. Toler-Franklin, D. Nehab, M. Burns, D. Dobkin, A. Vlachopoulos, C. Doumas, S. Rusinkiewicz, and T. Weyrich, "A system for high-volume acquisition and matching of fresco fragments: Reassembling Theran wall paintings," ACM Transactions on Graphics (Proc. SIGGRAPH), vol.27, no.3, Aug. 2008.
[5] P. Chen, M. Dai, K. Chen, and Z. Zhang, "Rotation axis calibration of a turntable using constrained global optimization," Optik - International Journal for Light and Electron Optics, vol.125, no.17, pp.4831–4836, 2014.
[6] J.H. Gao and L.-S. Peh, "A smartphone-based laser distance sensor for outdoor environments," 2016 IEEE International Conference on Robotics and Automation (ICRA), pp.2922–2929, May 2016.
[7] K. Konolige, J. Augenbraun, N. Donaldson, C. Fiebig, and P. Shah, "A low-cost laser distance sensor," 2008 IEEE International Conference on Robotics and Automation, pp.3002–3008, May 2008.
[8] R. Lenz and D. Fritsch, "Accuracy of videometry with ccd sensors," Isprs Journal of Photogrammetry and Remote Sensing, vol.45, no.2, pp.90–110, 1990.
[9] D. Li, H. Zhang, Z. Song, D. Man, and M.W. Jones, "An automatic laser scanning system for accurate 3D reconstruction of indoor scenes," 2017 IEEE International Conference on Information and Automation (ICIA), pp.826–831, July 2017.
[10] Y. Li, X. Fan, N.J. Mitra, D. Chamovitz, D. Cohen-Or, and B. Chen, "Analyzing growing plants from 4d point cloud data," ACM Trans. Graph., vol.32, no.6, pp.157:1–157:10, Nov. 2013.
[11] V. Matiukas and D. Miniotas, "Detection of laser beam's center-line in 2d images," Electronics and Electrical Engineering, vol.95, no.7, pp.67–70, 2009.
[12] Z. Niu, K. Liu, Y. Wang, S. Huang, X. Deng, and Z. Zhang, "Calibration method for the relative orientation between the rotation axis and a camera using constrained global optimization," Measurement Science and Technology, vol.28, no.5, 055001, 2017.
[13] X. Pang, R.W.H. Lau, Z. Song, Y. Li, and S. He, "A tool-free calibration method for turntable-based 3d scanning systems," IEEE Computer Graphics and Applications, vol.36, no.1, pp.52–61, Jan. 2016.
[14] S.-Y. Park and M. Subbarao, "A multiview 3d modeling system based on stereo vision techniques," Machine Vision and Applications, vol.16, no.3, pp.148–156, May 2005.
[15] D.F. Rogers and J.A. Adams, Mathematical Elements for Computer Graphics, second edition, McGraw-Hill Publishing Company, 1990.
[16] H. Rushmeier, J. Gomes, F. Giordano, H. El Shishiny, K. Magerlein, and F. Bernardini, "Design and use of an in-museum system for artifact capture," 2003 Conference on Computer Vision and Pattern Recognition Workshop, vol.1, p.8, June 2003.
[17] Y. Ye and Z. Song, "An accurate 3d point cloud registration approach for the turntable-based 3d scanning system," 2015 IEEE International Conference on Information and Automation, pp.982–986, Aug. 2015.
[18] D. York, "Least-squares fitting of a straight line," Canadian Journal

of Physics, vol.44, no.5, pp.1079–1086, 1966.
[19] Z. Zhang, "A flexible new technique for camera calibration," IEEE Trans. Pattern Anal. Mach. Intell., vol.22, no.11, pp.1330–1334, 2000.

Duhu Man received the M.S. and Ph.D. degrees in information engineering from Hiroshima University, Japan, in 2010 and 2013, respectively. He is currently a Research Fellow in Swansea University, UK. His research interests include parallel algorithm and image processing.

Mark W. Jones received the B.Sc. and Ph.D. degrees from Swansea University. He is a Professor in the Department of Computer Science at Swansea University, where he leads the Visual Computing Research group. His research interests include global illumination, visualisation, data science, and associated algorithms and data structures.

Danrong Li received his M.S. degree in computer science from the University of Science and Technology of China, Hefei, China, in 2018. His research interests include structured-light-based sensing, image processing, and calibration of 3d scanning system.

Honglong Zhang received his M.S. degree in computer science from Shenzhen Institutes of Advanced Technology, Chinese Academy of Sciences, Shenzhen, China, in 2018. His research interests include structured-light-based sensing, image processing, and calibration of 3d scanning system.

Zhan Song received his Ph.D. in mechanical and automation engineering from Chinese University of Hong Kong, Hong Kong, in 2008. He is currently with the Shenzhen Institutes of Advanced Technology, CAS, as a professor. His current research interests include structured-light-based sensing, image processing, 3-D face recognition, and human-computer interaction.